Food Bioprocess Technol (2014) 7:307–323
DOI 10.1007/s11947-013-1193-6

REVIEW

Recent Advances in Wavelength Selection Techniques for Hyperspectral Image Processing in the Food Industry

Dan Liu · Da-Wen Sun · Xin-An Zeng

Received: 2 July 2013 / Accepted: 15 September 2013 / Published online: 2 October 2013

Abstract During the past decade, hyperspectral imaging (HSI) has been rapidly developing and widely applied in the food industry by virtue of the use of chemometric techniques in which wavelength selection methods play an important role. This paper is a review of such variable selection methods and their limitations, describing the basic taxonomy of the methods and their respective advantages and disadvantages. Special attention is paid to recent developments in wavelength selection techniques for HSI in the field of food quality and safety evaluations. Typical and commonly used methods in HSI, such as partial least squares regression, stepwise regression and spectrum analysis, are described in detail. Some sophisticated methods, such as successive projections algorithm, uninformative variable elimination, simulated annealing, artificial neural network and genetic algorithm methods, are also discussed. Finally, new methods not currently used but that could have substantial impact on the field are presented. In short, this review provides an overview of wavelength selection methods in food-related areas and offers a thoughtful perspective on future potentials and challenges in the development of HSI systems.

Keywords Wavelength selection · Hyperspectral imaging · Multispectral · Food · Chemometrics

D. Liu · D.-W. Sun (✉) · X.-A. Zeng
College of Light Industry and Food Sciences, South China University of Technology, Guangzhou 510641, People's Republic of China
e-mail: dawen.sun@ucd.ie
URL: www.ucd.ie/refrig; www.ucd.ie/sun

D.-W. Sun
Food Refrigeration and Computerised Food Technology, Agriculture and Food Science Centre, University College Dublin, National University of Ireland, Belfield, Dublin 4, Ireland

Introduction

Originally developed for remote sensing applications, hyperspectral imaging (HSI) has recently found increasingly widespread use in non-destructive quality and safety inspection of food products, especially for the comprehensive testing of internal and external measures of quality for a wide variety of food and agricultural products. Hyperspectral imaging, also referred to in literature as spectroscopic imaging, imaging spectroscopy or chemical imaging, is a technique that combines the advantages of conventional digital imaging or computer vision (Wang and Sun 2002; Sun and Brosnan 2003a, b; Du and Sun 2005a, b; Jackman et al. 2008, 2009; Valous et al. 2009) and spectroscopy to simultaneously obtain both spatial and spectral information from an object (Sun 2010). This unique capability makes HSI especially attractive for straightforward, speedy evaluation of chemical (Mendoza et al. 2011; Barbin et al. 2013a), microbiological (Siripatrawan et al. 2011; Barbin et al. 2012b; Menesatti et al. 2013a) and quality attributes (Menesatti et al. 2009; Liu et al. 2011; Barbin et al. 2012a) of food products. In addition, the technique is useful for addressing some authenticity issues (Costa et al. 2011; Barbin et al. 2012c; Zhu et al. 2012) in the food industry.

A typical c.onfiguration of a HSI system consists of a light source to illuminate the object to be analysed, a lens to insure adequate focus and to delimit the field of view, a wavelength dispersion device (such as an imaging spectrograph) to split the light into various spectral bands, and a detector (such as a charge-coupled device or a camera) to capture the resultant spatial–spectral images. Generally, HSI analysis involves the rapid collection of a substantial number of hyperspectral images, each composed of two spatial dimensions and one spectral dimension. The useful information contained in these large hyperspectral images needs to be processed and extracted in order to predict the relevant quality attributes. However, the large size of such

hyperspectral data sets often complicates the process of predicting the value of a dependent variable.

One way to overcome this problem is to implement the HSI technique in conjunction with multivariate methods to decrease data size by identifying a few key wavelengths for rapid and accurate quantitative or qualitative analysis of food quality (Burger and Gowen 2011). Variable (wavelength) selection in multivariate analysis is an important step because the removal of highly correlated variables produces better prediction and a simpler process. Wavelength selection techniques usually consist of choosing from the full spectrum the small subset of significant wavelengths that carry the most important spectral information. This approach reduces the complexity of the data and improves the predictive capability of the model. In addition, the selection of key wavelengths saves overall time for the analysis, making the model more suited for online automated quality control systems. Using a few well-selected key wavelengths may be equally or even more efficient than using the full range of wavelengths in producing robust calibration models that are simple, cost-effective and amenable to automated industrial applications (Wold et al. 1996).

Recently, considerable effort has been made in developing procedures that identify key wavelengths for use in robust models in the food industry. There are many approaches available for selecting wavelengths for food analysis (Workman et al. 1996; Esbensen 2002). Typical wavelength selection methods, such as partial least squares regression (PLSR) and stepwise regression (SWR) (Chong and Jun 2005), are widely used for identifying key wavelengths in HSI analysis to assess quality of foods and agricultural products. For example, Kamruzzaman et al. (2013a) selected four wavelengths at 940, 1,067, 1,144 and 1,217 nm by PLSR for discrimination of pork from minced lamb, and Cluff et al. (2008) used SWR to identify seven key wavelengths in the visible and near-infrared (Vis-NIR) region (501, 510, 646, 651, 927, 1,005 and 1, 023 nm) in a HSI system to predict beef tenderness. The performance of these models based on optimal wavelengths was equally or even more efficient than those based on the result from the full spectrum of wavelengths. Other authors (Jouan-Rimbaud et al. 1995; Cai et al. 2008; Galvão et al. 2008; Chang 2011) have also explored the feasibility of using more sophisticated methods, such as successive projections algorithm (SPA), uninformative variable elimination (UVE), simulated annealing (SA), artificial neural network (ANN) and genetic algorithm (GA), for selecting appropriate wavelengths in robust HSI systems applied to numerous food commodities.

Several reviews (Balabin and Smirnov 2011; Zou et al. 2010a) have been published on wavelength selection methods in NIR spectroscopy. Additional reviews on feature selection methods and their application in classification are also available (Jain and Zongker 1997; Guyon and Elisseeff 2003). However, until now no review has been available on wavelength selection methods for use in HSI systems applied in the food industry. Therefore, this paper describes the most common wavelength selection techniques and presents some of the more recently developed methods for use with HSI systems in the fields of food quality and safety evaluation.

Hyperspectral and Multispectral Imaging Systems

Hyperspectral and multispectral imaging are the two of the four classes of spectral analysis that also include panchromatic and ultraspectral imaging that have witnessed tremendous growth over the past few years in the analysis of food. The spectral resolution is the main factor that distinguishes hyperspectral from multispectral imagery (Vagni 2007). Hyperspectral sensors contain bands with very high spectral resolution (10–20 nm), providing a more continuous spectral measurement across defined parts of electromagnetic spectrum. Multispectral sensors, on the other hand, contain broad bands with lower spectral resolution and are, therefore, less sensitive to subtle variations in reflected energy. However, the image acquisition time, complexity and purchase price of HSI systems are generally significantly higher than those associated with multispectral systems (Park et al. 2011). Therefore, HSI with a limited number of selected wavelengths represents a promising alternative to meeting the needs of real-time image acquisition and processing for the industry.

A Brief Overview of HSI Analysis

The concepts of hyperspectral and conventional imaging differ in the number of spectral bands used during image acquisition and data processing. Hyperspectral systems collect images in several contiguous and/or regularly spaced bands while conventional imaging systems operate at visible wavelengths in the form of monochromatic or discrete colour images (red, green and blue). Therefore, hyperspectral imaging produces a fuller spectrum of wavelength information for each pixel of the image. However, the combination of spectral and spatial data in the hypercube renders multidimensional data processing more complex than the conventional image analysis. The most commonly used hyperspectral analyses include classification and segmentation (Du and Sun 2004) or spectral analysis (Geladi and Dabakk 1995). For instance, several machine learning and image processing techniques have been employed to extract relevant information from hyperspectral data (Sun 2010). Currently, many spectral-based techniques, such as partial least square (PLS), principal component analysis (PCA), ANN and spectral angle mapper, are available to tackle the voluminous hyperspectral data sets (Menesatti et al. 2010; Liu et al. 2013). However, most hyperspectral data processing techniques focus on analyzing the spectral data without incorporating the spatial information.

The integration of spatial and spectral data has recently been shown to enhance the prediction accuracy of HSI (Mendoza et al. 2011). This fusion of the spatial and spectral information is an important part for hyperspectral analyses (Plaza et al. 2009).

Importance of Wavelength Selection in HSI Processing

Chemical and Physical Basis

NIR spectroscopy provides complex structural information related to the molecular bonds, such as O–H, C–H and N–H (Table 1). These bonds are subject to vibrational energy transfers when irradiated with electromagnetic frequencies in the NIR spectral range from 700 to 2,500 nm (Ghosh and Jayas 2009). Because of the complicated nature of NIR spectra involving large molecules, most NIR band assignments are made on an empirical basis. In complex mixtures, such as foods, the presence of multiple bands and the effect of peak-broadening result in NIR spectra with broad envelopes and few sharp peaks. In addition to information about the sample, the NIR spectra also contain background noise. To obtain reliable, accurate and stable calibration models, it is necessary to correct for the non-linearity by mathematical signal treatments, such as multiplicative scatter correction, standard normal variate or derivative absorption spectra (Rinnan et al. 2009). Judicious selection of wavelengths decreases sensitivity to non-linearity and discarding those uninformative wavelengths can expedite data processing and improve model accuracy and robustness.

Multivariate Calibration and Classification

From a multivariate calibration perspective, the problem of multicollinearity among contiguous variables (wavelengths, in this case) makes variable selection necessary. In many situations, variable selection can improve model performance and model characteristics (e.g. higher speed and greater cost-effectiveness) by identifying and removing useless, noisy and redundant variables. Variable selection also plays an important role in discriminant analysis and classification process. For example, construction of chemometric classification models with selected feature wavelengths by means of PLS–discriminant analysis (PLS-DA) (Papetti et al. 2012; Serranti et al. 2013), soft independent modeling of class analogy (Menesatti et al. 2013b) and linear discrimanant analysis (Wang et al. 2012b) yields good classification results. Variable selection procedures not only enhance discriminant performance but also facilitate the design of innovative HSI systems for quality control and/or separation purposes. The algorithms for calibration, prediction, classification and other data manipulation routines can be implemented through the use of software packages (e.g. MATLAB, ENVI and PARVUS) that are available for HSI processing in the food industry.

Table 1 Approximate location of Vis-NIR absorption bands of various chemical bonds

	C–H	N–H	O–H
Combination	2,300	2,200	2,000
1st overtone	1,745	1,540	1,450
2nd overtone	1,210	1,040	960
3rd overtone	934	785	730
4th overtone	762	–	–

Instrument and Industrial Requirements

Although HSI provides more spectral information than simpler multispectral images, its rather high price prohibits its widespread application. Appropriate wavelength selection can facilitate the establishment of consistent hyperspectral imaging systems with simple structure, short acquisition time and low cost for real-time applications.

Classification of Variable Selection Methods

Variable selection is defined as a process that chooses a minimum subset of M variables from an original set of N variables, so that the variable space is optimally reduced according to a certain evaluation criteria. The variable selection frame proposed by Dash and Liu (1997) include four steps (Fig. 1): (1) generation of a subset of candidates, (2) evaluation of the subset, (3) development of a criterion for deciding when to stop the selection procedure and (4) validation of the subset. There are three main variable selection methods: filter methods, wrapper methods and embedded methods. Table 2 provides a common taxonomy of variable selection methods, showing advantages and disadvantages of each technique (Saeys et al. 2007; Ladha and Deepa 2011).

Filter Methods

Filter methods evaluate the quality of selected features, independent of the classification algorithm (Fig. 2). In most cases, a feature-related score is calculated and the low-scoring features are eliminated. The resulting subset of features is used as input to the classification algorithm. Filter techniques have the advantages of being simple, fast and independent of the classification algorithm. A common disadvantage of such methods is the unknown interaction between feature subset search and classification algorithm. Some multivariate filter techniques have been developed to overcome this disadvantage, e.g. information gain (Ben-Bassat 1982) and correlation-based feature selection (CFS) (Hall 1999).

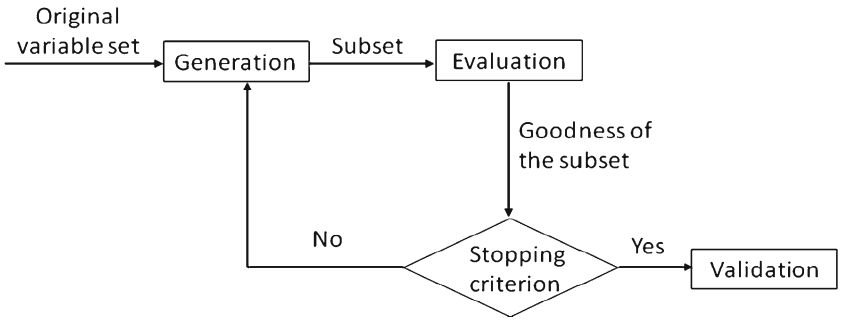

Fig. 1 Variable selection procedure (Dash and Liu 1997)

Wrapper Methods

In contrast to filter methods, wrapper methods require application of a classifier to evaluate its quality. Wrapper methods utilize the classifier as a black box to score the subsets of variables based on their predictive power (Fig. 3). Advantages of wrapper approaches include the interaction between feature subset search and model selection, and the ability to take feature dependencies into account. A common drawback of these techniques compared to filter techniques is the greater risk of overfitting and the more intensive computational burden. Learning algorithms, such as beam search (Siedelecky and Sklansky 1998), simulated annealing (Kirjpatrick et al. 1983) and genetic algorithms (Lavine 2006), are examples of wrapper methods.

Table 2 A taxonomy of variable selection techniques (Saeys et al. 2007)

Variable selection methods	Advantages	Disadvantages
Filter	Univariate	
	• Fast • Scalable • Independent of the classifier	✓ Ignoring variable dependencies ✓ Ignoring interaction with the classifier
	Multivariate	
	• Model variable dependencies • Independent of the classifier • Better computational complexity than wrapper methods	✓ Slower than univariate techniques ✓ Less scalable than univariate techniques ✓ Ignoring interaction with the classifier
Wrapper	Deterministic	
	• Simple • Interacting with the classifier • Model variable dependencies • Less computationally intensive than randomized methods	✓ Risk of over fitting ✓ More prone than randomized algorithms to getting stuck in a local optimum ✓ Classifier dependent selection
	Randomized	
	• Less prone to local optima • Interacting with the classifier • Model variable dependencies	✓ Computationally intensive ✓ Classifier dependent selection ✓ Higher risk of overfitting than deterministic algorithms
Embedded	• Interacting with the classifier • Better computational complexity than wrapper methods • Model variable dependencies	✓ Classifier dependent selection

Embedded Methods

In contrast to both filter and wrapper approaches, in embedded methods the learning part and the variable selection part interact, and the search for optimal variable is built into the classifier construction step (Fig. 4). Embedded methods have the advantages of simultaneously implementing training and variable selection processes and a reduced computational burden compared to wrapper methods. One of the limitations of these methods, however, is the dependency on classification algorithm. Traditional machine learning tools, such as decision trees (Duda et al. 2001) and support vector machine (SVM) (Guyon et al. 2002), are examples of embedded methods.

Wavelength Selection Methodologies in HSI Analysis

Partial Least Squares Regression and Stepwise Regression

Partial Least Squares Regression

The purpose of PLSR is to generate a linear model to predict a dependent response variable, y, from a large set of independent variables, X (e.g. a food quality predictor and wavelengths, in our case). Normally, there are two variable selection methods using PLS regression. The first one is to use variable importance in projection (VIP) scores (PLS-VIP method), and the other is to use regression coefficients estimated by PLS regression (PLS-β method) (Chong and Jun 2005). The underlying principles of the PLS-β method are introduced below because it is more widely used in wavelength selection for HSI analysis in the food industry.

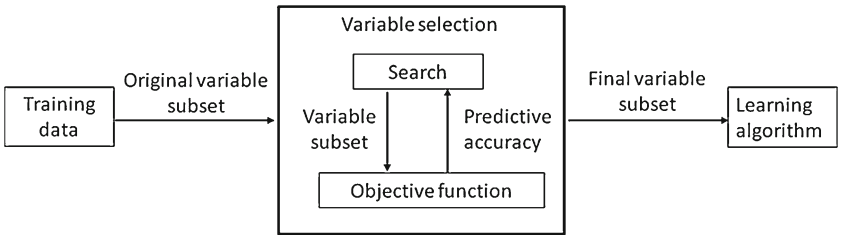

Fig. 2 Principle of filter method

Generally, the PLSR model with a set of orthogonal factors called latent variables (LVs) can be expressed as follows (Wold et al. 2001):

$$X = TP^T + E \quad (1)$$

$$y = Tq^T + f \quad (2)$$

$$T = XW^* \, where \, W^* = W\left(P^T W\right)^{-1} \quad (3)$$

where X is a $n \times m$ spectral matrix (n is the number of samples, m is the number of wavelengths), T is the wavelength scores, P is the $m \times k$ matrix of X loadings and q is the y loadings ($1 \times k$) (k is the number of latent variables), and y is the reference data ($n \times 1$) that needs to be predicted from X. E and f stand for random errors in X and y, respectively, while W is PLS weights, and W^* is the $m \times k$ matrix of X weights.

The regression coefficients (β) can be calculated from the PLS weights resulting from the model and the optimal number of LVs:

$$\beta = W^* q^T = W\left(P^T W\right)^{-1} q^T \quad (4)$$

The PLS model can be re-organized for k number of LVs and directly calculated by Eq. (4). The relevant predictors could be selected based on the magnitude of the absolute values of regression coefficients.

$$y^{\wedge} = XW_k\beta = T\beta \quad (5)$$

β is the vector containing the regression coefficients ($m \times 1$) obtained by the calibration model, while $\hat{y}$ is the predicted value of the attribute of interest.

β-coefficients obtained from the PLS calibration model are used for selecting the optimal wavelengths. The wavelengths corresponding to the highest absolute values of β-coefficients (i.e. regardless of sign) are selected as the optimal wavelengths.

Some wavelengths identified using PLSR in HSI analysis of food quality attributes are summarized in Table 3. The wavelengths selected by PLSR have been shown to yield similar and sometimes even better prediction accuracy than the PLS model that uses the full range of wavelengths (Barbin et al. 2012a, b, c, 2013a; Kamruzzaman et al. 2012a, b, 2013a; ElMasry et al. 2011, 2012, 2013). Examples of the use of selected wavelengths include prediction of various chemical parameters of meat (Table 3), specifically pork (Barbin et al. 2013a), beef (ElMasry et al. 2013), lamb (Kamruzzaman et al. 2012a) and Spanish cooked ham (Talens et al. 2013). These wavelengths selected based on PLSR β-coefficients not only produced stable prediction models but also favoured the easier implementation of potential multispectral imaging systems.

In addition to chemical composition assessments, HSI analysis has also been used to evaluate attributes of quality. The most important quality characteristics that determine the acceptability of food are appearance (colour, shape), odour, flavour, tenderness and firmness. Recently, colour parameters ($L^*a^*b^*$) in different types of meat such as pork (Barbin et al. 2012a), turkey ham (Iqbal et al. 2013), beef (ElMasry et al. 2012) and lamb (Kamruzzaman et al. 2012b) have been predicted by the same HSI system in the spectral range of 900–1,700 nm. PLS-β-coefficients were used to identify the important wavelengths, which yielded relatively good prediction accuracy (R^2>0.88) for all the meats. It is also interesting to note that for the same equipment, the same methods and the same parameters tested, different combinations of wavelengths were selected for different types of meat, such as L^* for pork, beef and lamb (Table 3). HSI has also been used extensively to predict tenderness, water holding capacity (WHC) and pH values of muscle foods. ElMasry et al. (2012) predicted fresh beef tenderness with a coefficient of determination (R^2_{cv}) of 0.77 based on 15 important wavelengths identified by β-coefficients from PLSR models in a

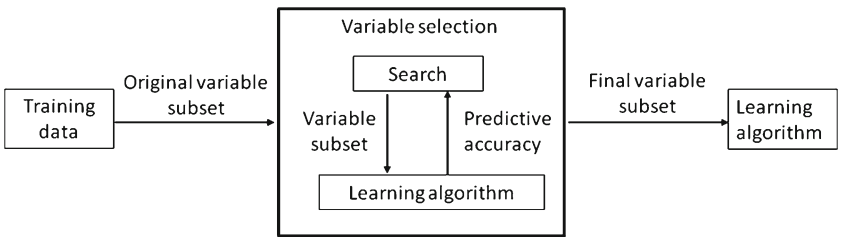

Fig. 3 Principle of wrapper method

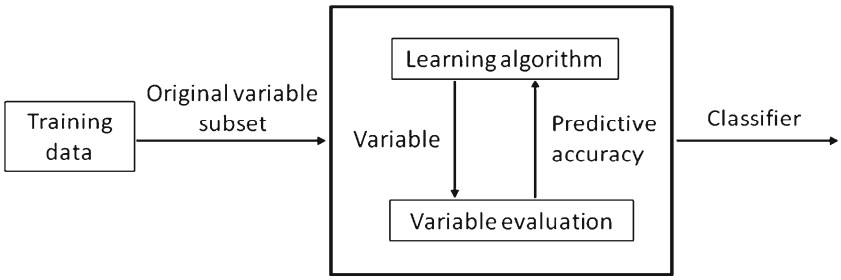

Fig. 4 Principle of embedded method

pushbroom HSI system (900–1,700 nm). WHC in pork (Barbin et al. 2012a) and beef (ElMasry et al. 2011) have also been evaluated. Seven and six wavelengths were used to predict WHC for pork and beef, resulting in R^2_{cv} values of 0.87 and 0.83, respectively (Table 3). Recently, pH has been predicted in fresh meat using HSI and the PLSR model. Good performances for predicting pH in pork (R^2_c=0.87, R^2_{cv}=0.86, R^2_p=0.90) were obtained by picking five important wavelengths at 947, 1,057, 1,161, 1,308 and 1,680 nm. Satisfactory PLSR models were also used to predict pH in fresh beef based on 24 wavelengths (R^2_{cv}=0.71) (ElMasry et al. 2012). In summary, by appropriate selection of wavelengths, it is possible to make good predictions of pH in meat, which suggests the possibility of replacing a meter with a fast and precise multispectral instrument.

A number of studies have also been undertaken to investigate the potential use of HSI for microbiological evaluation (Sivertsen et al. 2011; Barbin et al. 2012b; Feng et al. 2013) and categorization and authentication of food products (Sone et al. 2012; Kamruzzaman et al. 2013a; Barbin et al. 2013b). Feng et al. (2013) explored using HSI in combination with PLSR for the detection of *Enterobacteriaceae* (EB) loads on chicken fillets. The least squares support vector machines (LS-SVM) regression model with three wavelengths (930, 1,121 and 1,345 nm) selected by β-coefficients of PLSR was able to predict EB loads with R^2 values of 0.89, 0.86 and 0.87 for calibration, cross-validation and prediction, respectively. More recently, PLSR has been used to select four wavelengths (487, 606, 646 and 980 nm) for separating fresh cod fillets from frozen–thawed ones in a HSI system (Sivertsen et al. 2011). For the authentication of meat products, a HSI system in the NIR range (900–1,700 nm) was exploited for the classification of fresh Atlantic salmon fillets stored under different atmospheres (Sone et al. 2012). Five wavelengths (606, 636, 665, 705 and 764 nm) were identified and a classification accuracy of >88 % was achieved, based on *K*-nearest neighbor classifier. In another application of the method, Kamruzzaman et al. (2013a) developed a predictive model using PCA to identify adulteration in pork, as well as kidney, heart and lung in minced lamb. In this case, four important wavelengths (940, 1,067, 1,144 and 1,217 nm) were selected using PLSR and an optimized multiple linear regression (MLR) prediction model resulted in R^2_{cv} of 0.98. Furthermore, PLS-DA models based on 13 optimal wavelengths that were selected using PLS-β-coefficients were successfully used to distinguish between fresh and frozen–thawed porcine longissimus dorsi muscles with an overall correct classification of 100 % (Barbin et al. 2013b).

While the majority of studies have focused on selecting feature wavelengths by PLSR for muscle foods, some attempts have also been made to use this method for estimating quality and safety parameters of agricultural products (ElMasry et al. 2008; Bhuvaneswari et al. 2011; Rajkumar et al. 2012; Zhang and He 2013). For example, a HSI system was developed employing three wavelengths in the NIR region (750, 820, 960 nm) selected by PLSR and used for early detection of bruises on apples. (ElMasry et al. 2008). Recently, banana fruit quality was distinguished at different stages of maturity using MLR models to identify eight optimal wavelengths (Fig. 5). R^2_{cv} values of 0.85, 0.87 and 0.91 were found for total soluble solids, moisture and firmness of the banana fruits, respectively. These data indicate that HSI can be used as a non-destructive method for evaluating banana fruit ripening/maturity stages (Rajkumar et al. 2012). In another study, Bhuvaneswari et al. (2011) developed a HSI system to detect insect fragments in semolina, in which ten wavelengths were identified by the β-coefficients of PLSR. Another study (Zhang and He 2013) used hyperspectral images of oilseed rape leaves in Vis-NIR region (380–1,030 nm) for the early estimation of seed yield. In this case, an optimized PLSR model based on six key wavelengths (543, 686, 718, 741, 824 and 994 nm) performed well (R^2_P=0.71, RMSEP=23.72) for predicting seed weight, thereby demonstrating the potential of HSI to estimate seed yield in early growing stage.

Stepwise Regression

SWR is a useful procedure for selecting key wavelengths, particularly when a large number of variables are involved. It performs the modeling by analysing a large number of variables and selecting those that fit well. The approaches to variable selection by SWR can be classified into three methods: forward selection (forward addition), backward selection (backward elimination) and stepwise selection (Wang and Jain 2003). The forward selection and backward elimination methods are also sometimes called gradient methods

Table 3 Feature wavelengths identified using PLSR and SWR in hyperspectral imaging analysis for predicting food quality attributes

Methods	Applications	Selected wavelengths (nm)	No.	References
PLSR	WC of pork	927, 950, 1,047, 1,211, 1,325, 1,513, 1,645	7	Barbin et al. (2013a)
	Fat of pork	927, 937, 990, 1,047, 1,134, 1,211, 1,275, 1,382, 1,645	9	
	Protein of pork	927, 940, 994, 1,051, 1,084, 1,138, 1,181, 1,211, 1,275, 1,325, 1,645	11	
	WHC of pork	940, 990, 1,054, 1,108, 1,208, 1,311, 1,650	7	Barbin et al. (2012a)
	pH of pork	947, 1,057, 1,161, 1,308, 1,680	5	
	*L** of pork	947, 1,024, 1,124, 1,208, 1,268, 1,654	6	
	*a** of pork	944, 964, 1,057, 1,120, 1,181, 1,211, 1,267, 1,368, 1,398, 1,501, 1,631	11	
	*b** of pork	964, 1,064, 1,161, 1,211, 1,274, 1,648	6	
	PPC in pork	947, 1,118, 1,128, 1,151, 1,211, 1,241, 1388, 1,621, 1,641, 1,655	10	Barbin et al. (2012b)
	Recognition of Fresh and F-T pork	928, 938, 944, 957, 970, 1,030, 1,053, 1,080, 1,108, 1,170, 1,178, 1,225 , 1,383, 1,645	13	Barbin et al. (2013b)
	WC of beef	934, 1,048, 1,108, 1,155, 122 1,185, 1,212, 1,265, 1,379	8	ElMasry et al. (2013)
	Fat of beef	934, 978, 1,078, 1,138, 1,215, 1,289, 1,413	7	
	Protein of beef	924, 937, 1,018, 1,048, 1,108, 1,141, 1,182, 1,221, 125 1,615, 1,665	10	
	Tenderness of beef	927, 941, 974, 1,034, 1,084, 1,105, 1,135, 1,175, 1,218, 1,249, 1,285, 1,309, 1,571, 1,658, 1,682	15	ElMasry et al. (2012)
	*L** of beef	947, 1,078, 1,151, 1,215, 1,376, 1,645	6	
	pH of beef	924, 937, 951, 961, 984, 1,044, 1,091, 1,111, 1,117, 1,158, 1,245, 1,251, 1,285, 1,316, 1,342, 1,363, 1,376, 1,406, 1,413, 1,443, 1,476, 1,500, 1,524, 1,541	24	
	WHC of beef	940, 997, 1,144, 1,214, 1,342, 1,443	6	ElMasry et al. (2011)
	WC of lamb	960, 1,057, 1,131, 1,211, 1,308, 1,394	6	Kamruzzaman et al. (2012a)
	Fat of lamb	960, 1,057, 1,131, 1,211, 1,308, 1,394	6	
	Protein of lamb	1,008, 1,211, 1,315, 1,445, 1,562, 1,649	6	
	*L** of lamb	940, 980, 1,037, 1,104, 1,151, 1,258, 1,365, 1,418	8	Kamruzzaman et al. (2012b)
	Detect pork in minced lamb	940, 1,067, 1,144, 1,217	4	Kamruzzaman et al. (2013a)
	WC of ham	930, 971, 1,084, 1,212, 1,645 and 1,682	6	Talens et al. (2013)
	Protein of ham	930, 971, 1,051, 1,137, 1,165, 1,212, 1,295, 1,400, 1,645, 1,682	10	
	Classification of ham	966, 1,061, 1,148, 1,256, 1,373, 1,628	6	
	WC of turkey	927, 944, 1,004, 1,058, 1,108, 1,212, 1,259, 1,362, 1,406	9	Iqbal et al. (2013)
	pH of turkey	927, 947, 1,004, 1,071, 1,121, 1,255, 1,312, 1,641	8	
	*a** of turkey	914, 931, 991, 1,115, 1,164, 1,218, 1,282, 1,362, 1,638	9	
	Freshness detection in cod	487, 606, 646, 980	4	Sivertsen et al. (2011)
	Fresh salmon detection	606, 636, 665, 705, 764	5	Sone et al. (2012)
	EB in chicken	930, 1,121, 1,345	3	Feng et al. (2013)
	Bruises of apples	750, 820, 960	3	ElMasry et al. (2008)
	Banana fruit quality	440, 525, 633, 672, 709, 760, 925, 984	8	Rajkumar et al. (2012)
	Detect insect in semolina	1,070, 1,200, 1,220, 1,290, 1,330, 1,380, 1,410, 1,520, 1,540, 1,570	10	Bhuvaneswari et al. (2011)
	Estimation of seed yield	543, 686, 718, 741, 824, 994	6	Zhang and He (2013)
SWR	Tenderness of beef	501, 510, 646, 651, 927, 1,005, 1,023	7	Cluff et al. (2008)
	Tenderness of beef	485, 533, 680, 772	4	Peng and Wu (2008)
	Tenderness of beef	485, 524, 541, 645, 700, 720, 780, 820	8	Wu et al. (2012c)
	*L** of beef	653, 678, 722, 868, 875, 920, 1,050	7	
	*a** of beef	465, 575, 614, 635, 671, 724, 978	7	
	*b** of beef	486, 524, 540, 645, 700, 721, 780, 954	8	
	TVC in beef	596, 822, 838, 841, 889, 900	5	Peng et al. (2011)
	Tenderness of pork	612, 632, 708, 770, 786, 814	6	Tao et al. (2012)
	E. coli in Pork	525, 875, 858, 534, 530	5	
	TVC in pork	477, 509, 540, 552, 560, 609, 720, 772	8	Wang et al. (2011)
	TVC in chicken	1,145, 1,458, 1,522, 1,659, 1,666, 1,669, 1,972	7	Feng and Sun (2013a)
	Detecting foreign materials among blueberries	1,268, 1,317	2	Sugiyama et al. (2010)

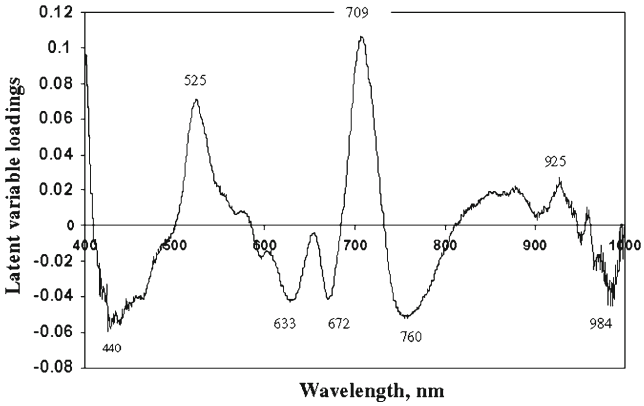

Fig. 5 Optimal wavelengths selected by PLSR for predicting quality attributes of banana fruits (Rajkumar et al. 2012)

since the addition or elimination step is performed on the basis of the steepest gradient of the error surface. As a combination of forward and backward methods, SWR is a more general method for selecting variables by adding variables when they are significant, and removing them when they are not. The main steps of stepwise method are listed below (Montgomery et al. 2001):

(1) Calculating simple correlation coefficients (r_{yx}) with the following equation, and then selecting the first variable having largest r_{yx} to enter into the model (X_1);

$$r_{yx} = \frac{\sum\left(Y-\overline{Y}\right)\left(X-\overline{X}\right)}{\sqrt{\sum\left(Y-\overline{Y}\right)^2}\sqrt{\sum\left(X-\overline{X}\right)^2}} \quad (6)$$

(2) Given that X_1 is already in the model, calculating r_{yx1x2} between Y and the remaining X variables by the equation below, and then selecting the second variable (X_2) having highest r_{yx1x2} for inclusion in the model;

$$r_{yx_1x_2} = \frac{r_{yx_2} - r_{yx_1}r_{x_1x_2}}{\sqrt{\left(1-r_{yx_1}^2\right)\left(1-r_{x_1x_2}^2\right)}} \quad (7)$$

(3) Dropping variable X_1 if the F test indicates that coefficient of X_1 is insignificant;
(4) Recalculating and selecting the highest partial correlation coefficient between Y and the remaining X variables for inclusion in the model;
(5) Repeating steps (3) and (4) to test all remaining variables, including those variables dropped at earlier stages, until the best subset of independent variables is selected.

This stepwise algorithm has been used for the wavelength selections in HSI systems by several authors (Table 3). Some researchers have attempted to use the SWR method to identify the key wavelengths from the hyperspectral image data to predict WBSF values of beef and pork: e.g., 501, 510, 646, 651, 927, 1,005 and 1,023 nm (Cluff et al. 2008); 485, 533, 680 and 772 nm (Peng and Wu 2008); 485, 524, 541, 645, 700, 720, 780 and 820 nm (Wu et al. 2012a); or 612, 632, 708, 770, 786 and 814 nm (Tao et al. 2012). These wavelengths are associated with myoglobin and its different forms, which are highly correlated with measured WBSF values. These studies demonstrate the suitability of this variable selection technique for predicting meat tenderness by HSI. In addition, Wu et al. (2012c) developed hyperspectral scattering profiles for predicting colour parameters (L^*, a^*, b^*) of 7-day-aged beef. Seven wavelengths for L^*, seven for a^* and eight for b^* were identified by SWR (Table 3). With these key wavelengths as the input of MLR model, the best prediction was obtained with R_{cv} of 0.96, 0.96 and 0.97 for L^*, a^* and b^*, respectively. For predicting *Escherichia coli* in pork, Tao et al. (2012) applied a SWR approach to identify five optimal wavelengths (525, 875, 858, 534 and 530 nm) as inputs for MLR. Their results gave an R_{cv} of 0.84 and RMSECV of 1.07, indicating good prediction of *E. coli* contamination in pork. For the detection of total viable count (TVC) in beef, Peng et al. (2011) explored the use of a HSI system (600–1,000) in a scattering mode. The MLR validation models gave the highest R^2_p of 0.95 with the lowest RMSEP of 0.30 for TVC based on six optimal wavelengths (596, 822, 838, 841, 889 and 900 nm). Similarly, Wang et al. (2011) investigated the potential use of HSI, in combination with LS-SVM, for detecting TVC of bacteria in pork meat. The performance of the developed LS-SVM model was good (R^2_{cv}=0.92 and RMSECV= 0.33) when using seven important wavelengths. Feng and Sun (2013a) reported on a good model for quantitative and direct determination of TVC in raw chicken fillets (R^2_{cv}=0.94 and residual predictive deviation (RPD)=3.02) using only seven wavelengths (1,145, 1,458, 1,522, 1,659, 1,666, 1,669 and 1, 972 nm) selected via SWR. In a recent study, the stepwise forward selection method was used to identify two important wavelengths (1,268 and 1,317 nm) for differentiating blueberries from foreign substances in a NIR spectral imaging system. Foreign materials were clearly distinguished from blueberries by applying the discriminant function and a threshold value to the absorbance images based on these two wavelengths (Sugiyama et al. 2010).

Successive Projections Algorithm and Uninformative Variable Elimination

Successive Projections Algorithm

The SPA is a variable selection algorithm designed to select wavelengths with minimal redundant information. SPA employs a simple projection operation in a vector space to select subsets of variables with a minimum of colinearity (Martens and Naes 1993). The candidate variable selected by SPA has the maximum projection value on the orthogonal subspace of the previous selected variable. Basically, SPA involves three

main steps (Galvão et al. 2008). The first step consists of projections on the columns of the spectral matrix, which generate candidate subsets of variables with minimum colinearity. The second step involves evaluating candidate subsets of variables based on the value of root mean square error (RMSE) obtained from validation set of MLR calibration. The final step aims to remove uninformative variables by a variable elimination procedure without significant loss of prediction capability.

Good results involving the use of SPA together with multivariate analysis have been reported in HSI analyses (Table 4). Wu et al. (2012a) developed a long wavelength near-infrared HSI system for predicting colour parameters (L^*, a^*, b^*) of salmon fish in which SPA was employed to select optimal wavelengths. Three predictive effective wavelengths for L^*, three for a^* and seven for b^* were identified and resulted in correlation coefficients (R_{cv}) of 0.876, 0.744 and 0.803, respectively. The same researchers also investigated the use of the SPA method for wavelength selection in water/moisture content predictions of prawns (Wu et al. 2012b) and beef (Wu et al. 2013) in a visible-NIR HSI system. Twelve optimal wavelengths were selected for moisture content prediction of prawns and six were selected for beef, with results of R^2_p=0.97 and RPD=5.17 for prawns and R^2_{cv}= 0.95 and RMSECV=1.28 % for beef (see Table 4). Recently, researchers have reported on the use of the SPA method for wavelengths selection in the non-destructive assessment of instrumental and sensory tenderness of lamb meat (Kamruzzaman et al. 2013b). In this study, 11 wavelengths were identified as being most related to instrumental tenderness (Table 4). Based on these wavelengths, a reasonably accurate prediction (R_{cv}=0.84) and categorization (89 %) of lamb meat was obtained. The SPA method has also been applied to wavelength selection for dynamic observation of peroxidase (POD) activity and growth state of tomatoes (Fang et al. 2012). With eight wavelengths (443, 464, 413, 410, 401, 402, 426 and 926 nm) determined by the SPA method, the model gave an R_p of 0.94 and RMSEP of 37.80. This result shows the feasibility of determining the POD activity with an optimized HSI system to obtain predictions of satisfactory accuracy. However, one disadvantage of variables selection by SPA is its low signal to noise ratio (S/N) or insufficiency in multivariate calibration, both of which can negatively affect the accuracy of the model prediction. To reduce this limitation, SPA has been favourably combined with other algorithms, such as uninformative variable elimination (Ye et al. 2008) and genetic algorithm (Zou et al. 2010b).

Uninformative Variable Elimination

UVE is a method for variable selection based on an analysis of regression coefficients of PLS (Centner 2009). In the PLSR prediction model, there is a relationship between X (spectral matrix) and Y (concentration matrix):

$$Y = Xb + e \tag{8}$$

where b is the regression coefficient vector and e is the error vector.

The principle of the algorithm is to add an artificial random matrix with a small amplitude to the original spectral matrix to form a new matrix and carry out leave-one-out-cross-validation between the new matrix and concentration matrix Y (Centner et al. 1996). After each step of leave-one-out-cross-validation, a regression coefficient matrix b is obtained. Because each coefficient, b_i, represents the contribution of the corresponding variable to the established model, the reliability of each variable i can be quantitatively measured by the stability defined as:

$$C_i = \frac{\text{mean}(b_i)}{\text{std}(b_i)} \tag{9}$$

where mean(b_i) and std(b_i) are the mean value and standard deviation of the regression coefficients of the ith wavelength,

Table 4 Feature wavelengths identified using SPA and UVE in hyperspectral imaging analysis for predicting food quality attributes

Methods	Applications	Selected wavelengths (nm)	No.	References
SPA	L^* of salmon	1,161, 1,295, 1,362	3	Wu et al. (2012a)
	a^* of salmon	1,081, 1,161, 1,362	3	
	b^* of salmon	964, 1,024, 1,081, 1,105, 1,161, 1,295, 1,362	7	
	WC of prawn	428, 445, 544, 569, 629, 672, 20 697, 760, 827, 917, 958, 999	12	Wu et al. (2012b)
	WC of beef	518, 669, 761, 874, 989, 1,030	6	Wu et al. (2013)
	Tenderness of lamb	934, 964, 1,017, 1,081, 1,144, 1,215, 1,265, 1,341, 1,455, 1,615, 1,655	11	Kamruzzaman et al. (2013b)
	Detection of activity of POD in tomato leaves	443, 464, 413, 410, 401, 402, 426, 926	8	Fang et al. (2012)
UVE	Predict apple firmness	525, 530, 600, 605, 630, 635, 640, 650, 655, 660, 690, 695, 710, 735, 755, 765, 800, 805, 810, 830, 840, 845, 850, 855, 870, 900, 905, 910, 920, 945, 950, 985, 990, 995	34	Wang et al. (2012a)

respectively. The absolute value of C_i is used to determine if each wavelength in the spectrum improves the result or not. A large C_i is a measure of the importance of the corresponding wavelength. If the Ci is below a threshold level, then wavelength i is treated as uninformative and is eliminated. The remaining wavelengths are used to create a new independent variable matrix. This new matrix and Y are then used to establish a new PLSR prediction model.

The UVE algorithm has been applied in wavelength selections in NIR spectroscopy, achieving good prediction results (Shao et al. 2004; Cai et al. 2008). However, few studies have investigated the use of the UVE algorithm in HSI analysis. In the first attempt in this regard, Wang et al. (2012a) investigated a model fusion method that used UVE algorithms for the prediction of apple firmness in a hyperspectral scattering imaging system. Figure 6 shows the stability of wavelengths in the range of 500–1,000 nm in the calibration set using UVE. The two horizontal dotted lines represent the lower and upper thresholds. Based on the UVE principle, the wavelengths whose stabilities lie outside the dotted lines were selected as optimal wavelengths. In this study, 34 wavelengths were selected as the input of the PLS model. The results of the UVE-PLS model were better than those of the PLS model using all of the wavelengths. This fusion model combined the advantages of the two algorithms, eliminating the limitation of the single algorithm and giving improved predictions of apple firmness.

Spectrum Derivative and Band Ratio

Another way to select optimal wavelengths is by visually observing the spectral profile and selecting the wavelengths manually. The spectral bands not only contain chemical/physical information but also maintain the discrimination and classification efficiency. Second derivative and band ratio algorithms have been used for dimensionality reduction and identification of the most important wavelengths (Savitzky and Golay 1964). In the case of second derivative spectra, the wavelengths selected were in regions of the spectrum where there were great spectral differences among the tested samples. For the band ratio approach, wavelengths were determined by the ratio of the responses at two different spectral bands. Both derivative spectra and band ratio approaches can reduce the multiplicative effect and intensify the spectral signals related to the chemical composition of samples.

Ratio features and spectral analysis have been successfully used for selecting wavelengths in many food inspection applications (Table 5). Kamruzzaman et al. (2012c) examined categorization and authentication of longissimus dorsi muscle of red meat (pork, beef and lamb) and identified from second derivative spectra six significant wavelengths using PLS-DA which yielded an overall classification accuracy of 98.67 % (Table 5). More recently, a HSI system in the NIR range (900–1,700 nm) was exploited for classifying pork samples as "fresh" or "spoiled" (Barbin et al. 2012b). Seven optimal wavelengths were selected by second derivative of average spectra and used to classify the tested samples with an accuracy of 95 % using linear discriminant analysis. In another study, three quality grades, i.e. RFN (reddish-pink, firm and non-exudative), PSE (pale/pinkish-gray, soft and exudative) and DFD (dark purplish red, firm and dry) of longissimus dorsi muscle in pork were classified with an accuracy of 96 % using PCA with only six wavelengths (960, 1,074, 1,124, 1,147, 1,207 and 1,341 nm) identified from second derivative spectra (Barbin et al. 2012c). In a recent study, Feng et al. (2013) used the second derivative-based method for selecting key wavelengths in a HSI system to elucidate the changes in *Enterobacteriaceae* loads in chicken fillets. Four important wavelengths (948, 960, 1,134 and 1,144 nm) were selected and yielded good results, although not as good as the result of a full wavelength model. Chao et al. (2008) developed a pushbroom Vis-NIR spectral imaging system for distinguishing between wholesome and diseased chickens. Four optimal wavelengths (424, 465, 515 and 546 nm) for differentiating between wholesome and systemically diseased chickens were selected by spectrum analysis, which achieved classification accuracies of greater than 90 %, indicating the possibility of implementing multispectral line-scan operation. Furthermore, the second derivative method was conducted on the absorbance data of fresh, fast frozen–thawed and slow frozen–thawed fish. The spectral changes (at 970, 729, 836, 928, 552, 512 and 620 nm) observed led to a clear distinction between the samples (Zhu et al. 2012).

Several authors have used the band ratio method of identifying optimal wavelengths for purposes of product defect detection and characterization. Li et al. (2010) investigated the potential of using HIS for detecting canker lesions on citrus fruit. Wavelengths of 630, 685 and 720 nm were identified for use in this study. The dual-band reflectance ratio (such as Q720/685) algorithm was performed on images of navel oranges to differentiate canker from normal fruit skin and other surface diseases. An overall classification success rate of almost 97 % was obtained. Jiang et al. (2011) investigated the feasibility of using HSI data to detect infected areas on citrus surfaces in the wavelength range between 500 and 950 nm. Optimum index factor method was applied to identify the optimal wavelength combination, yielding a 97.5 % classification rate. In a different application, Nakariyakul and Casasent (2011) introduced a successful method for detecting internally damaged almonds using only two sets of ratio features (850/1,210 nm, 1,160/1,335 nm) in a hyperspectral transmission mode (Fig. 7).

Other Wavelength Selection Methods

In addition to the more commonly used wavelength selection methods described above, some other algorithms for applications in HSI analysis have been developed recently. The

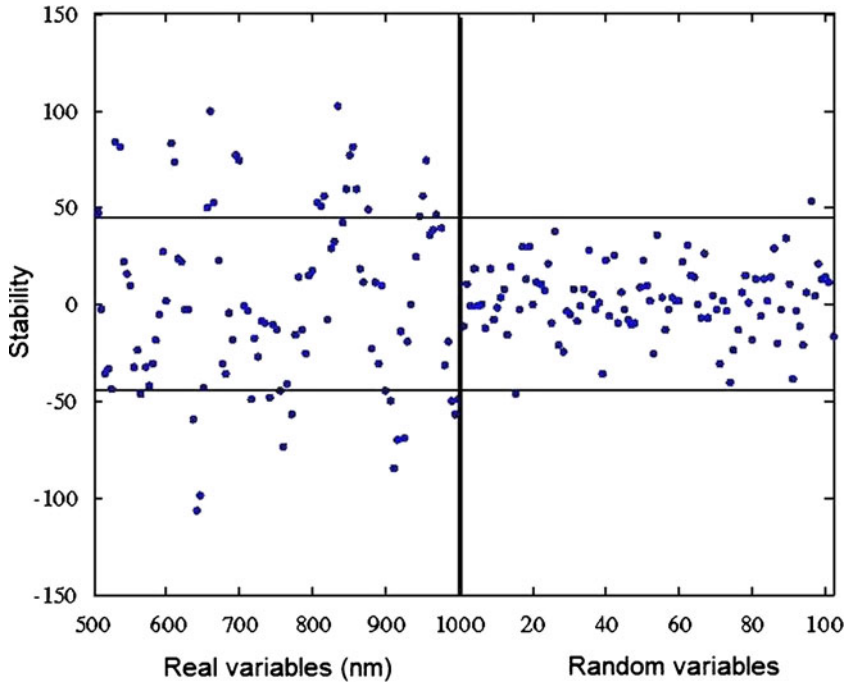

Fig. 6 Selecting wavelengths using the UVE algorithm for predicting apple firmness (Wang et al. 2012a)

following section provides a brief overview of the applications of these methods in HSI for quality evaluation of foodstuffs (Table 6). Among these methods, ANN has been fully developed for quantitative analysis of food samples. ANN is designed to mimic the structure of biological neural networks. In a biological application, the approach consists of modeling a system of one or more hidden layers of neurons that receive several input values and produces a single output. When applied to selection of optimal wavelengths, the approach seeks the optimal set of wavelengths inputs that can successfully predict or classify the single desired output. Another method is to calculate the causal index (CI) of the trained ANN model (Glorfeld 1996). The higher the CI value, the more important the node is for the classification or prediction. ElMasry et al. (2009) developed feed-forward back propagation ANN models to select optimal wavelengths for the detection of chilling injury in Red Delicious apples. Five optimal wavelengths at 717, 751, 875, 960 and 980 nm yielded an average classification accuracy of 98.4 % for distinguishing normal and injured fruits.

Another new method is SA, which is a probabilistic global optimization technique based on the annealing process in metallurgy (Kirjpatrick et al. 1983). Swierenga et al. (1998) demonstrated that variable selection by SA enhanced the model's robustness and also improved its predictive capability. This method has also been applied to hyperspectral data sets for feature extraction (Fang et al. 2006; Chang 2011). However, application of the SA wavelength selection method to problems of quality prediction in the food industry has rarely been reported possibly due to the instability of this method and the considerable level of expertise required for users to adjust the numerous factors of the algorithm.

The GA is another newly developed method for analysing NIR spectra, which employs a probabilistic, non-local search

Table 5 Feature wavelengths identified using spectrum derivative and band ratio in hyperspectral imaging analysis for predicting food quality attributes

Methods	Applications	Selected wavelengths (nm)	No.	References
2nd D	Categorization of red meat	957, 1,071, 1,121, 1,144, 1,368, 1,394	6	Kamruzzaman et al. (2012c)
	Grading of pork *LD*	960, 1,074, 1,124, 1,147, 1,207, 1,341	6	Barbin et al. (2012c)
	Spoilage detection in pork	964, 1,128, 1,151, 1,301, 1,341, 1,395, 1,635	7	Barbin et al. (2012b)
	Determination of *Enterobacteriaceae* on chicken	948, 960, 1,134, 1,144	4	Feng et al. (2013)
	Disease detection in chicken	440, 460, 500, 540, 580, 620	6	Chao et al. (2008)
	Differentiate fresh and frozen–thawed fish	970, 729, 836, 928, 552, 512, 620	7	Zhu et al. (2012)
Band ratio	Detecting Citrus canker	630, 685, 720	3	Li et al. (2010)
	Detection of infected *Tephritidae* citrus fruit	500, 950	2	Jiang et al. (2011)
	Classification of internally damaged almond nuts	850/1,210, 1,160/1,335	4	Nakariyakul and Casasent (2011)

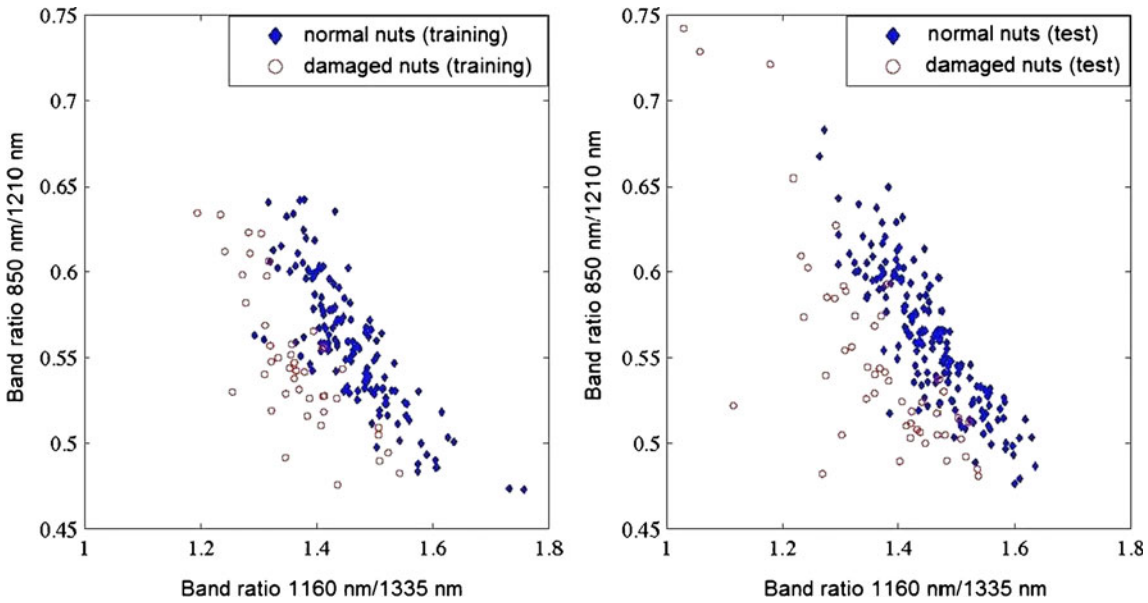

Fig. 7 Plot of the training (**a**) and test (**b**) set samples for the two best sets of ratio features chosen by band ratio method for classification of internally damaged almond nuts (Nakariyakul and Casasent 2011)

process inspired by Darwin's theory of natural selection (Jouan-Rimbaud et al. 1995). GA is capable of exploring the space of all possible subsets in a reasonable amount of time. The development of GA for analysis of spectral data has been reported in detail by Lavine et al. (2000, 2002). The GA algorithm is developing rapidly and has been recently applied to selection of optimum wavelengths in HSI systems, For example, Wallays et al. (2009) found the best combinations of a few wavebands (465–475, 522–532, 676–705, 849–858 and 906–945 nm) for successful classification of kernel or material other-than-grain in wheat. Additionally, wavelength selection schemes based on GA were investigated for direct and rapid determination of *Pseudomonas* loads in raw chicken breast fillets in a pushbroom HSI system (Feng and Sun 2013b). The selected wavelengths in the five regions, i.e. 1,138–1,155, 1,195–1,198, 1,392–1,395, 1,452–1,455 and 1,525–1,529 nm, led to a prediction model with R^2>0.87 and RMSE<0.65 log10 CFU g^{-1}, illustrating the promising capability of HSI for microbiological evaluation of meat products. Gómez-Sanchis et al. (2008) detected rottenness caused by *Penicillium* genus fungi in citrus fruits using machine learning techniques. The classification accuracy was above 91 % using a reduced set of 20 optimally selected bands by GA (Table 6).

Some other new wavelength selection methods in HSI analysis have also been investigated, such as competitive adaptive reweighted sampling (CARS) (Wu and Sun 2013),

Table 6 Feature wavelengths identified using other methods in hyperspectral imaging analysis for predicting food quality attributes

Methods	Applications	Selected wavelengths (nm)	No.	References
ANN	Chilling injury in Red Delicious apple	717, 751, 875, 960, 980	5	ElMasry et al. (2009)
GA	Measurement of grain cleanness	465–475, 522–532, 676–705, 849–858, 906–945	5	Wallays et al. (2009)
	Pseudomonas loads in chicken fillets	1,138–1,155, 1,195–1,198, 1,392–1,395, 1,452–1, 455, 1,525–1,529	5	Feng and Sun (2013b)
	Detection of rottenness caused by *Penicillium digitatum* in mandarins	460, 480, 520, 560, 590, 600, 620, 630, 680, 730, 740, 760, 800, 820, 870, 880, 950, 960, 980, 1,010	20	Gómez-Sanchis et al. (2008)
CARS	Microbial spoilage of salmon flesh	495, 535, 550, 585, 625, 660, 785, 915	8	Wu and Sun (2013)
ROC	Detection of bruises on apples	808, 760, 832, 772, 834, 762, 788, 742	8	Luo et al. (2012)
BB	Internal defect of pickling cucumbers	745, 805, 965, 985	4	Ariana and Lu (2010)
	Poultry skin tumor detection	482, 496, 513, 518, 556, 575, 729, 733	8	Nakariyakul and Casasent (2009)
MRMR	Detecting rottenness caused in citrus	650, 720, 700, 740, 930, 530, 770, 710, 480, 460	10	Gomez-Sanchis et al. (2012)
	Classification of decay in mandarins	650, 720, 700, 740, 930, 530, 770, 710, 480, 460	10	Gomez-Sanchis et al. (2013)

ANN artificial network, *GA* genetic algorithm, *ROC* receiver operating characteristic, *CARS* competitive adaptive reweighted sampling, *BB*, branch and bound, *MRMR* minimum redundancy maximum relevance

receiver operating characteristic (ROC) analysis (Luo et al. 2012), branch and bound (BB) algorithm (Nakariyakul and Casasent 2009; Ariana and Lu 2010) and minimum redundancy-maximum relevance (MRMR) (Gomez-Sanchis et al. 2012a, 2013). These methods have been used to successfully select the optimal wavelengths, leading to robust prediction models. For instance, by using the CARS method, eight optimal wavelengths were identified for predicting TVC of salmon flesh with a coefficient of determination (R^2_p) of 0.985 and RPD of 5.13 (Wu and Sun 2013). ROC analysis was used to select effective wavelengths in the range of 380–1,000 nm to detect bruises in four cultivars of apples. With the highest AUC (area under the ROC curve) value, the best wavelength pairs for Fuji, Jonagold, Orin and Sinano Gold cultivars were centered at $R(808)$–$R(760)$, $R(832)$–$R(772)$, $R(834)$–$R(762)$ and $R(788)$–$R(742)$, respectively (Fig. 8). The classification accuracies using optimal wavelengths determined by PLS-DA were comparable to those resulting from the use of the full range of wavelengths (Luo et al. 2012). Another new algorithm BB has been used recently by Ariana and Lu (2010) to identify two sets of four wavelengths (i.e. 745, 805, 965, 985 nm and of 745, 765, 885, 965 nm) for damage detection of pickling cucumbers and whole pickles, respectively. Classification accuracies of 94.7 and 82.9 % were achieved in this study. In another application, an adaptive branch and bound algorithm (ABB) was used by Nakariyakul and Casasent (2009) to select featured wavelength for poultry skin tumour detection in a HSI system. The use of ABB resulted in the detection of more skin tumours than visual inspection and with fewer false alarms. Only eight wavebands were required to detect 32 out of 40 poultry skin tumors. These data are promising for eventual commercialization of online applications because many fast multispectral sensor systems are capable of recording up to eight wavebands.

Recently, the MRMR method has been proposed to select wavelengths with minimum redundancy. The method assesses which feature has the highest correlation with the class feature (maximal relevance), and at the same time, it calculates the information that is shared with the remainder of features using

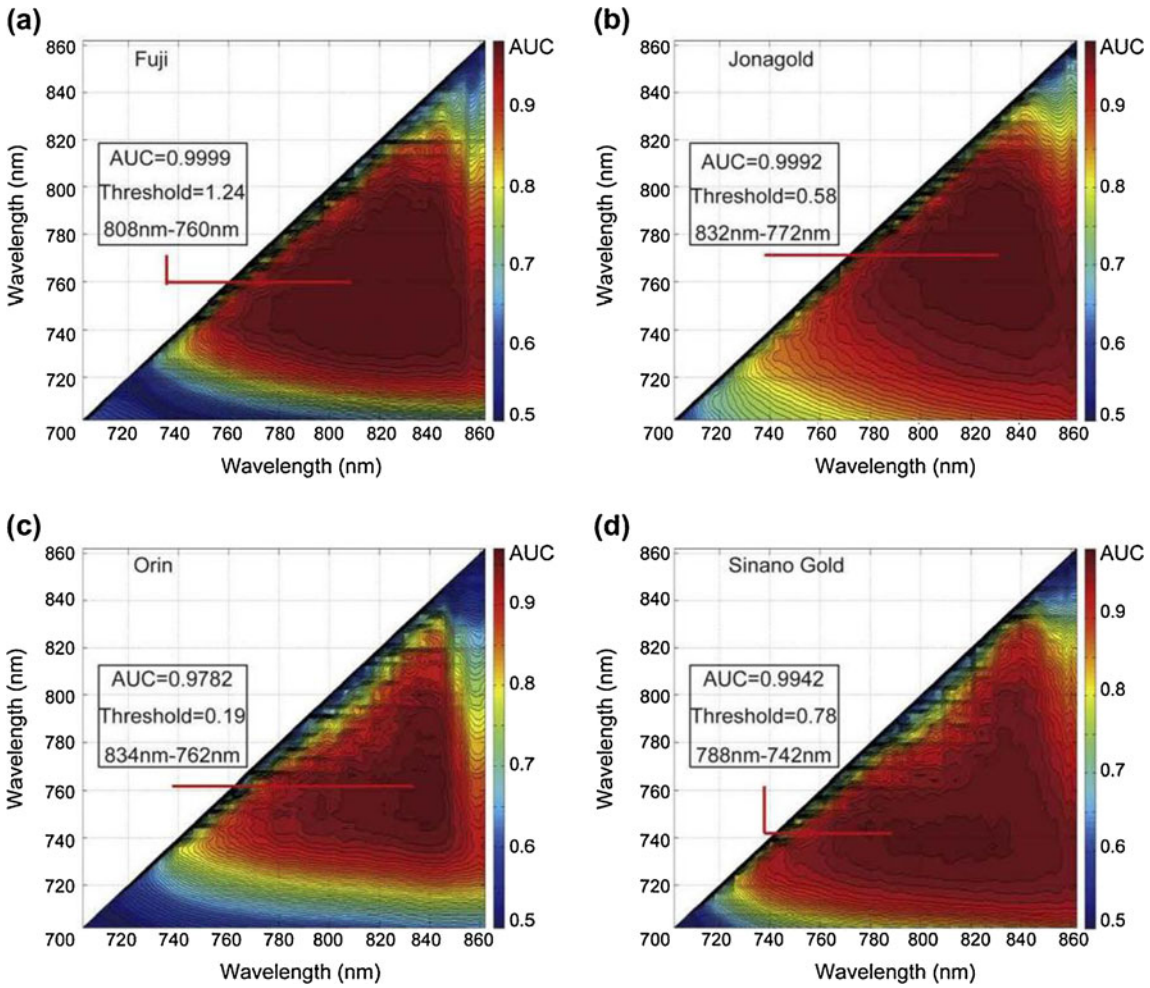

Fig. 8 AUC (area under the ROC curve) values of all possible combinations of two wavelengths ($R(\lambda_1)$–$R(\lambda_2)$) in the 700–860 nm waveband. The pair of wavelengths that received the highest AUC value was selected as the best pair. **a** Fuji. **b** Jonagold. **c** Orin. **d** Sinano Gold (Luo et al. 2012)

mutual information (minimum redundancy). By doing this, MRMR expands the representative power of the feature set and improves its generalization properties (Ponsa and Lopez 2007). MRMR has been used to select relevant features to detect rottenness caused by *Penicillium* genus fungi in citrus fruits (Gomez-Sanchis et al. 2012) and to classify decay in mandarins caused by *Penicillium digitatum* and *Penicillium italicum* (Gomez-Sanchis et al. 2013) (Table 6). Based on these suitable numbers of wavelengths, an accuracy of around 98 and 93 % was achieved for rottenness detection and decay classification, respectively. The results indicated the suitability of the proposed approach.

In spite of the methodologies currently used in HSI, additional methods used in pattern recognition of spectral analysis could have substantial impact on hyperspectral data analysis. The potential applications of filter methods ranges from simple univariate interactions to more advanced multivariate methods, such as CFS, Markov blanket filter and fast correlation-based feature selection, which could highlight the advantage of using univariate and multivariate filter procedures in spectral feature extraction domain. Also, variable selection using wrapper (sequential forward selection, sequential backward elimination, beam search) or embedded methods (decision trees, naive Bayes, SVM) could also offer alternative approaches to performing a multivariate spectral subset selection, incorporating the classifier's bias into the search and thus offering an opportunity to construct more accurate prediction models.

Conclusions

Because a HSI system produces voluminous amounts of data, it often requires careful and sophisticated processing in order to extract the most relevant information. Careful selection of optimal wavelengths can be very useful in extracting useful information from these hyperspectral data and improving performance of multivariate calibration models. Applying wavelength selection methods to HSI data in applications such as food quality evaluation, food safety and adulteration detection can greatly improve prediction results. Several wavelength selection approaches have been discussed in this review including PLSR, SWR, spectrum analysis, SPA and UVE. The principles and applications of these different algorithms to hyperspectral analysis usually lead to different results. Therefore, there is no single, universally optimal technique for selecting key wavelengths in a general case. The choice of a particular method depends on the nature of the problem, the size of the dataset, ease of implementation and required accuracy of prediction.

Considering the emerging technical challenges and future potentials in the design of HSI systems, improvements are needed to address the issue of the length of time needed for image acquisition and data analysis, both of which limit the application of these approaches to real-time, online systems. As an alternative, a common multispectral imaging system with a limited number of wavebands has the capability to meet the needs of real-time acquisition and processing. Appropriate selection of important wavelengths plays an important role in further exploitation of HSI systems. All of the wavelengths selection methods summarized in this review can provide a basis for the design and development of a fast, reliable and accurate multispectral imaging system for online, real-time applications. The high image acquisition speed in combination with effective wavelength selection techniques have the potential to bring online sorting of foods within reach.

Despite so many research efforts for developing multispectral imaging systems for quality, safety and authenticity of foods by means of the above-mentioned selection techniques, there are still some challenges to be dealt with. Specifically, further research is needed to focus on analyzing the hyperspectral data with integrated univariate and sequential algorithms to take advantage of the complementarities that both sources of information can provide. Moreover, the tentative attempt of new variable selection methods (e.g. multivariate filter method, beam search and weighted naive Bayes) that currently are not being used in HSI analysis could be meaningful.

Acknowledgments The authors are grateful to the Guangdong Province Government (China) for support through the program of "Leading Talent of Guangdong Province (Da-Wen Sun)". This research was also supported by China Postdoctoral Science Foundation (2013M530366). Prof Don and Karen Barnes and Dr Rana Muhammad Aadil are gratefully acknowledged for kind assistance and revisions of English quality and styling of this paper.

References

Ariana, D. P., & Lu, R. (2010). Hyperspectral waveband selection for internal defect detection of pickling cucumbers and whole pickles. *Computers and Electronics in Agriculture, 74*(1), 137–144.

Balabin, R. M., & Smirnov, S. V. (2011). Variable selection in near-infrared spectroscopy: benchmarking of feature selection methods on biodiesel data. *Analytica Chimica Acta, 692*(1–2), 63–72.

Barbin, D., ElMasry, G., Sun, D.-W., & Allen, P. (2012a). Predicting quality and sensory attributes of pork using near-infrared hyperspectral imaging. *Analytica Chimica Acta, 719*, 30–42.

Barbin, D. F., ElMasry, G., Sun, D.-W., Allen, P., & Noha, M. (2012b). Non-destructive assessment of microbial contamination in porcine meat using NIR hyperspectral imaging. *Innovative Food Science & Emerging Technologies, 17*, 180–191.

Barbin, D., ElMasry, G., Sun, D.-W., & Allen, P. (2012c). Near-infrared hyperspectral imaging for grading and classification of pork. *Meat Science, 90*(1), 259–268.

Barbin, D. F., ElMasry, G., Sun, D.-W., & Allen, P. (2013a). Non-destructive determination of chemical composition in intact and minced pork by near-infrared hyperspectral imaging. *Food Chemistry, 138*(2–3), 1162–1171.

Barbin, D. F., Sun, D.-W., & Su, C. (2013b). NIR hyperspectral imaging as non-destructive evaluation tool for the recognition of fresh and

frozen-thawed porcine longissimus dorsi muscles. *Innovative Food Science & Emerging Technologies, 18*, 226–236.

Ben-Bassat, M. (1982). Pattern recognition and reduction of dimensionality. In: Krishnaiah P. and Kanal L. (eds.) Handbook of statistics II, Vol. 1. North-Holland, Amsterdam. pp. 773–791.

Bhuvaneswari, K., Fields, P. G., White, N. D. G., Sarkar, A. K., Singh, C. B., & Jayas, D. S. (2011). Image analysis for detecting insect fragments in semolina. *Journal of Stored Products Research, 47*, 20–24.

Burger, J., & Gowen, A. (2011). Data handling in hyperspectral image analysis. *Chemometrics and Intelligent Laboratory Systems, 108*, 13–22.

Cai, W., Li, Y., & Shao, X. (2008). A variable selection method based on uninformative variable elimination for multivariate calibration of near-infrared spectra. *Chemometrics and Intelligent Laboratory Systems, 90*, 188–194.

Centner, V., Massart, D. L., & De Noord, O. E. (1996). Elimination of uninformative variables for multivariate calibration. *Analytical Chemistry, 68*(21), 3851–3858.

Centner, V. (2009). Multivariate approaches: UVE-PLS. *Chemistry and Biochemistry Data Analysis, 21*, 609–618.

Chang, Y.-L. (2011). A simulated annealing feature extraction approach for hyperspectral images. *Future Generation Computer Systems, 27*(4), 419–426.

Chao, K., Yang, C., Kim, M., & Chan, D. (2008). High throughput spectral imaging system for wholesomeness inspection of chicken. *Applied Engineering in Agriculture, 24*(4), 475–485.

Chong, I. G., & Jun, C. H. (2005). Performance of some variable selection methods when multicollinearity is present. *Chemometrics and Intelligent Laboratory Systems, 78*(1–2), 103–112.

Cluff, K., Naganathan, G. K., Subbiah, J., Lu, R., Calkins, C. R., & Samal, A. (2008). Optical scattering in beef steak to predict tenderness using hyperspectral imaging in the VIS-NIR region. *Sensing and Instrumentation for Food Quality and Safety, 2*(3), 189–196.

Costa, C., D'Andrea, S., Russo, R., Antonucci, F., Pallottino, F., & Menesatti, P. (2011). Application of non-invasive techniques to differentiate sea bass (*Dicentrarchus labrax, L. 1758*) quality cultured under different conditions. *Aquaculture International, 19*(4), 765–778.

Dash, M., & Liu, H. (1997). Feature selection for classification. *Intelligent Data Analysis, 1*, 131–156.

Du, C.-J., & Sun, D.-W. (2004). Recent developments in the applications of image processing techniques for food quality evaluation. *Trends in Food Science & Technology, 15*, 230–249.

Du, C.-J., & Sun, D.-W. (2005a). Comparison of three methods for classification of pizza topping using different colour space transformations. *Journal of Food Engineering, 68*(3), 277–287. doi:10.1016/j.jfoodeng.2004.05.044.

Du, C.-J., & Sun, D.-W. (2005b). Pizza sauce spread classification using colour vision and support vector machines. *Journal of Food Engineering, 66*(2), 137–145. doi:10.1016/j.jfoodeng.2004.03.011.

Duda, R., Hart, P., & Stork, D. (2001). *Pattern classification*. New York: Wiley.

ElMasry, G., Wang, N., Vigneault, C., Qiao, J., & ElSayed, A. (2008). Early detection of apple bruises on different background colors using hyperspectral imaging. *LWT–Food Science and Technology, 41*(2), 337–345.

ElMasry, G., Wang, N., & Vigneault, C. (2009). Detecting chilling injury in Red Delicious apple using hyperspectral imaging and neural networks. *Postharvest Biology and Technology, 52*(1), 1–8.

ElMasry, G., Sun, D.-W., & Allen, P. (2011). Non-destructive determination of water-holding capacity in fresh beef by using NIR hyperspectral imaging. *Food Research International, 44*(9), 2624–2633.

ElMasry, G., Sun, D.-W., & Allen, P. (2012). Near-infrared hyperspectral imaging for predicting colour, pH and tenderness of fresh beef. *Journal of Food Engineering, 110*(1), 127–140.

ElMasry, G., Sun, D.-W., & Allen, P. (2013). Chemical-free assessment and mapping of major constituents in beef using hyperspectral imaging. *Journal of Food Engineering, 117*(2), 235–246.

Esbensen, K. H. (2002). *Multivariate data analysis in practice* (5th ed.). Oslo: CAMO Process.

Fang, H., Zou, Q., He, Y., & Li, X. L. (2012). Detection of activity of POD in tomato leaves based on hyperspectral imaging technology. *Spectroscopy and Spectral Analysis, 32*(8), 2228–2233.

Fang, J.P., Chang, Y.L., Ren, H., Lin, C.C., Liang, W.Y., & Fang, J.F. (2006). A simulated annealing band selection approach for hyperspectral imagery. *Proceedings of SPIE 6378*, doi:10.1117/12.685683.

Feng, Y.-Z., ElMasry, G., Sun, D.-W., Scannell, A. G. M., Walsh, D., & Morcy, N. (2013). Near-infrared hyperspectral imaging and partial least squares regression for rapid and reagentless determination of *Enterobacteriaceae* on chicken fillets. *Food Chemistry, 138*(2–3), 1829–1836.

Feng, Y.-Z., & Sun, D.-W. (2013a). Determination of total viable count (TVC) in chicken breast fillets by near-infrared hyperspectral imaging and spectroscopic transforms. *Talanta, 105*, 244–249.

Feng, Y.-Z., & Sun, D.-W. (2013b). Near-infrared hyperspectral imaging in tandem with partial least squares regression and genetic algorithm for non-destructive determination and visualization of *Pseudomonas* loads in chicken fillets. *Talanta, 109*, 74–83.

Galvão, R. K. H., Araújo, M. C. U., Fragoso, W. D., Silva, E. C., José, G. E., Soares, S. F. C., et al. (2008). A variable elimination method to improve the parsimony of MLR models using the successive projections algorithm. *Chemometrics and Intelligent Laboratory Systems, 92*(1), 83–91.

Geladi, P., & Dabakk, E. (1995). An overview of chemometrics applications in near infrared spectrometry. *Journal of Near Infrared Spectroscopy, 3*(1), 119–132.

Ghosh, P. K., & Jayas, D. S. (2009). Use of spectroscopic data for automation in food processing Industry. *Sensing and Instrumentation for Food Quality and Safety, 3*, 3–11.

Glorfeld, L. W. (1996). A methodology for simplification and interpretation of back propagation-based neural network models. *Expert Systems with Applications, 10*(1), 37–54.

Gómez-Sanchis, J., Gómez-Chova, L., Aleixos, N., Camps-Valls, G., Montesinos-Herrero, C., Moltó, E., et al. (2008). Hyperspectral system for early detection of rottenness caused by *Penicillium digitatum* in mandarins. *Journal of Food Engineering, 89*(1), 80–86.

Gomez-Sanchis, J., Martin-Guerrero, J. D., Soria-Olivas, E., Martinez-Sober, M., Magdalena-Benedito, R., & Blasco, J. (2012). Detecting rottenness caused by *Penicillium genus fungi* in citrus fruits using machine learning techniques. *Expert Systems with Applications, 39*, 780–785.

Gomez-Sanchis, J., Blasco, J., Soria-Olivas, E., Lorente, D., Escandell-Montero, P., Martinez-Martinez, J. M., et al. (2013). Hyperspectral LCTF-based system for classification of decay in mandarins caused by *Penicillium digitatum* and *Penicillium italicum* using the most relevant bands and non-linear classifiers. *Postharvest Biology and Technology, 82*, 76–86.

Guyon, I., Weston, J., Barnhill, S., & Vapnik, V. (2002). Gene selection for cancer classification using support vector machines. *Machine Learning, 46*, 389–422.

Guyon, I., & Elisseeff, A. (2003). An introduction to variable and feature selection. *Journal of Machine Learning Research, 3*, 1157–1182.

Hall, M. (1999). Correlation-based feature selection for machine learning. PhD Thesis., Department of Computer Science, Waikato University, New Zealand.

Iqbal, A., Sun, D.-W., & Allen, P. (2013). Prediction of moisture, color and pH in cooked, pre-sliced turkey hams by NIR hyperspectral imaging system. *Journal of Food Engineering, 117*(1), 42–51.

Jain, A. K., & Zongker, D. (1997). Feature selection: evaluation, application, and small sample performance. *IEEE Transactions on Pattern Analysis and Machine Intelligence, 19*(2), 153–158.

Jackman, P., Sun, D.-W., Du, C.-J., Allen, P., Downey, G. (2008). Prediction of beef eating quality from colour, marbling and wavelet texture features. *Meat Science, 80*(4), 1273–1281. doi:10.1016/j.meatsci.2008.06.001.

Jackman, P., Sun, D.-W., Du, C.-J., Allen, P. (2009). Prediction of beef eating qualities from colour, marbling and wavelet surface texture features using homogenous carcass treatment. *Pattern Recognition, 42*(5), 751–763. doi:10.1016/j.patcog.2008.09.009.

Jiang, Y.L., Zhang, R.Y., Yu, J., Hu, W.C., & Yin, Z.T. (2011). Detection of infected *Tephritidae* citrus fruit based on hyperspectral imaging and two-band ratio algorithm. *Advanced Materials Research,* 311–313, 1501–1504.

Jouan-Rimbaud, D., Massart, D. L., Leardi, R., & De Noord, O. E. (1995). Genetic algorithms as a tool for wavelength selection in multivariate calibration. *Analytical Chemistry, 67*(23), 4295–4301.

Kamruzzaman, M., ElMasry, G., Sun, D.-W., & Allen, P. (2012a). Non-destructive prediction and visualization of chemical composition in lamb meat using NIR hyperspectral imaging and multivariate regression. *Innovative Food Science & Emerging Technologies, 16*, 218–226.

Kamruzzaman, M., ElMasry, G., Sun, D.-W., & Allen, P. (2012b). Prediction of some quality attributes of lamb meat using near infrared hyperspectral imaging and multivariate analysis. *Analytica Chimica Acta, 714*, 57–67.

Kamruzzaman, M., Barbin, D., ElMasry, G., Sun, D.-W., & Allen, P. (2012c). Potential of hyperspectral imaging and pattern recognition for categorization and authentication of red meat. *Innovative Food Science & Emerging Technologies, 16*, 316–325.

Kamruzzaman, M., Sun, D.-W., ElMasry, G., & Allen, P. (2013a). Fast detection and visualization of minced lamb meat adulteration using NIR hyperspectral imaging and multivariate image analysis. *Talanta, 103*, 130–136.

Kamruzzaman, M., ElMasry, G., Sun, D.-W., & Allen, P. (2013b). Non-destructive assessment of instrumental and sensory tenderness of lamb meat using NIR hyperspectral imaging. *Food Chemistry, 141*(1), 389–396.

Kirjpatrick, S., Gelatt, C. D., & Vecchi, M. P. (1983). Optimization by simulated annealing. *Science, 220*, 671–690.

Ladha, L., & Deepa, T. (2011). Feature selection methods and algorithms. *International Journal of Computational Engineering Science, 3*(5), 1787–1797.

Lavine, B. K., Ritter, J., Moores, A. J., Wilson, M., Faruque, A., & Mayfield, H. T. (2000). Source identification of underground fuel spills by solid-phase microextraction/high-resolution gas chromatography/genetic algorithms. *Analytical Chemistry, 72*(2), 423–431.

Lavine, B. K., Davidson, C. E., & Moores, A. J. (2002). Genetic algorithms for spectral pattern recognition. *Vibrational Spectroscopy, 28*(1), 83–95.

Lavine, B. K. (2006). Pattern recognition. *Critical Reviews in Analytical Chemistry, 36*(3–4), 153–161.

Li, J. B., Rao, X. Q., Guo, J. X., & Ying, Y. B. (2010). Hyperspectral reflectance imaging for detecting citrus canker based on dual-band ratio image classification method. 5th international symposium on advanced optical manufacturing and testing technologies. *Proceedings of SPIE*. doi:10.1117/12.867065.

Liu, D., Zeng, X.-A., & Sun, D.-W. (2013). Recent developments and applications of hyperspectral imaging for quality evaluation of agricultural products: a review. *Critical Reviews in Food Science and Nutrition*. doi:10.1080/10408398.2013.777020.

Liu, F., He, Y., Wang, L., & Sun, G. M. (2011). Detection of organic acids and pH of fruit vinegars using near-infrared spectroscopy and multivariate calibration. *Food and Bioprocess Technology, 4*(8), 1331–1340.

Luo, X., Takahashi, T., Kyo, K., & Zhang, S. (2012). Wavelength selection in vis/NIR spectra for detection of bruises on apples by ROC analysis. *Journal of Food Engineering, 109*(3), 457–466.

Martens, H., & Naes, T. (1993). *Multivariate Calibration*. London: Wiley.

Mendoza, F., Lu, R., Arianab, D., Cen, H., & Bailey, B. (2011). Integrated spectral and image analysis of hyperspectral scattering data for prediction of apple fruit firmness and soluble solids content. *Postharvest Biology and Technology, 62*(2), 149–160.

Menesatti, P., Zanella, A., D'Andrea, S., Costa, C., Paglia, G., & Pallottino, F. (2009). Supervised multivariate analysis of hyperspectral NIR images to evaluate the starch index of apples. *Food and Bioprocess Technology, 2*(3), 308–314.

Menesatti, P., Antonucci, F., Pallottino, F., Giorgi, S., Matere, A., Nocente, F., et al. (2013a). Laboratory vs. in-field spectral proximal sensing for early detection of *Fusarium* head blight infection in durum wheat. *Biosystems Engineering, 114*(3), 289–293.

Menesatti, P., Antonucci, F., Pallottino, F., Bucarelli, F. M., & Costa, C. (2013b). Spectrophotometric qualification of Italian pasta produced by traditional or industrial production parameters. *Food and Bioprocess Technology*. doi:10.1007/s11947-013-1138-0.

Menesatti, P., Costa, C., & Aguzzi, J. (2010). Quality evaluation of fish by hyperspectral imaging. In D.-W. Sun (Ed.), *Hyperspectral imaging for food quality: analysis and control* (pp. 273–294). London: Academic.

Montgomery, D. C., Peck, E. A., & Vining, G. G. (2001). *Introduction to linear regression analysis (3rd ed.)* (pp. 131–154). New York: Wiley.

Nakariyakul, S., & Casasent, D. P. (2009). Fast feature selection algorithm for poultry skin tumor detection in hyperspectral data. *Journal of Food Engineering, 94*(3–4), 358–365.

Nakariyakul, S., & Casasent, D. P. (2011). Classification of internally damaged almond nuts using hyperspectral imagery. *Journal of Food Engineering, 103*(1), 62–67.

Papetti, P., Costa, C., Antonucci, F., Figorilli, S., Solaini, S., & Menesatti, P. (2012). A RFID web-based infotracing system for the artisanal Italian cheese quality traceability. *Food Control, 27*(1), 234–241.

Park, B., Yoon, S.-C., Windham, W., Lawrence, K., Kim, M., & Chao, K. (2011). Line-scan hyperspectral imaging for real-time in-line poultry fecal detection. *Sensing and Instrumentation for Food Quality and Safety, 5*, 25–32.

Peng, Y., & Wu, J. (2008). Hyperspectral scattering profiles for prediction of beef tenderness. ASABE, Providence, Rhode Island, June 29–July 2.

Peng, Y., Zhang, J., Wang, W., Li, Y., Wu, J., Huang, H., et al. (2011). Potential prediction of the microbial spoilage of beef using spatially resolved hyperspectral scattering profiles. *Journal of Food Engineering, 102*(2), 163–169.

Plaza, A., Benediktsson, J. A., Boardman, J. W., Brazile, J., Bruzzone, L., Camps-Valls, G., et al. (2009). Recent advances in techniques for hyperspectral image processing. *Remote Sensing of Environment, 113*, S110–S122.

Ponsa, D., & Lopez, A. (2007). Feature selection based on a new formulation of the minimal redundancy-maximal-relevance criterion. Lecture notes in computer science. *Pattern Recognition and Image Analysis, 4477*, 47–54.

Rajkumar, P., Wang, N., EImasry, G., Raghavan, G. S. V., & Gariepy, Y. (2012). Studies on banana fruit quality and maturity stages using hyperspectral imaging. *Journal of Food Engineering, 108*(1), 194–200.

Rinnan, A., Berg, F., & Engelsen, S. B. (2009). Review of the most common pre-processing techniques for near-infrared spectra. *TrAC Trends in Analytical Chemistry, 28*(10), 1201–1222.

Saeys, Y., Inza, I., & Larranaga, P. (2007). A review of feature selection techniques in bioinformatics. *Bioinformatics, 23*(19), 2507–2517.

Savitzky, A., & Golay, M. J. E. (1964). Smoothing and differentiation of data by simplified least squares procedures. *Analytical Chemistry, 36*, 1627–1639.

Serranti, S., Cesare, D., Marini, F., & Bonifazi, G. (2013). Classification of oat and groat kernels using NIR hyperspectral imaging. *Talanta, 103*, 276–284.

Shao, X. G., Wang, F., Chen, D., & Su, Q. D. (2004). A method for near-infrared spectral calibration of complex plant samples with wavelet transform and elimination of uninformative variables. *Analytical and Bioanalytical Chemistry, 378*(5), 1382–1387.

Siedelecky, W., & Sklansky, J. (1998). On automatic feature selection. *International Journal of Pattern Recognition and Artificial Intelligence, 2*, 197–220.

Siripatrawan, U., Makino, Y., Kawagoe, Y., & Oshita, S. (2011). Rapid detection of *Escherichia coli* contamination in packaged fresh spinach using hyperspectral imaging. *Talanta, 85*, 276–281.

Sivertsen, A. H., Kimiya, T., & Heia, K. (2011). Automatic freshness assessment of cod (*Gadus morhua*) fillets by Vis/Nir spectroscopy. *Journal of Food Engineering, 103*(3), 317–323.

Sone, I., Olsen, R. L., Sivertsen, A. H., Eilertsen, G., & Heia, K. (2012). Classification of fresh Atlantic salmon (*Salmo salar L.*) fillets stored under different atmospheres by hyperspectral imaging. *Journal of Food Engineering, 109*(3), 482–489.

Sugiyama, T., Sugiyama, J., Tsuta, M., Fujita, K., Shibata, M., Kokawa, M., et al. (2010). NIR spectral imaging with discriminant analysis for detecting foreign materials among blueberries. *Journal of Food Engineering, 101*(3), 244–252.

Sun, D.-W. (2010). *Hyperspectral imaging for food quality analysis and control*. San Diego: Academic.

Sun, D.-W., & Brosnan, T. (2003a). Pizza quality evaluation using computer vision - part 1 - Pizza base and sauce spread. *Journal of Food Engineering, 57*(1), 81–89. doi:10.1016/S0260-8774(02)00275-3.

Sun, D.-W., & Brosnan, T. (2003b). Pizza quality evaluation using computer vision - part 2 - Pizza topping analysis. *Journal of Food Engineering, 57*(1), 91–95. doi:10.1016/S0260-8774(02)00276-5.

Swierenga, H., de Groot, P. J., de Weijer, A. P., Derksen, M. W. J., & Buydens, L. M. C. (1998). Improvement of PLS model transferability by robust wavelength selection. *Chemometrics and Intelligent Laboratory Systems, 41*(2), 237–248.

Talens, P., Mora, L., Morsy, N., Barbin, D. F., ElMasry, G., & Sun, D.-W. (2013). Prediction of water and protein contents and quality classification of Spanish cooked ham using NIR hyperspectral imaging. *Journal of Food Engineering, 117*(3), 272–280.

Tao, F., Peng, Y., Li, Y., Chao, K., & Dhakal, S. (2012). Simultaneous determination of tenderness and *Escherichia coli* contamination of pork using hyperspectral scattering technique. *Meat Science, 90*(3), 851–857.

Vagni, F. (2007). Survey of hyperspectral and multispectral imaging technologies. *RTO Technical Report*, TR-SET-065-P3.

Valous, N. A., Mendoza, F., Sun, D-W., Allen, P. (2009). Colour calibration of a laboratory computer vision system for quality evaluation of pre-sliced hams. *Meat Science, 81*(1), 132–141

Wallays, C., Missotten, B., De Baerdemaeker, J., & Saeys, W. (2009). Hyperspectral waveband selection for on-line measurement of grain cleanness. *Biosystems Engineering, 104*(1), 1–7.

Wang, H. H., & Sun, D.-W. (2002). Melting characteristics of cheese: analysis of effect of cheese dimensions using computer vision techniques. *Journal of Food Engineering, 52*(3), 279–284. doi:10.1016/S0260-8774(01)00116-9.

Wang, G. C., & Jain, C. L. (2003). *Regression analysis: modeling and forecasting*. Fresh Meadows: Graceway.

Wang, S., Huang, M., & Zhu, Q. (2012a). Model fusion for prediction of apple firmness using hyperspectral scattering image. *Computers and Electronics in Agriculture, 80*, 1–7.

Wang, W., Peng, Y., Huang, H., & Wu, J. (2011). Application of hyperspectral imaging technique for the detection of total viable bacteria count in pork. *Sensor Letters, 9*(3), 1024–1030.

Wang, W., Li, C., Tollner, E. W., Gitaitis, R. D., & Rains, G. C. (2012b). Shortwave infrared hyperspectral imaging for detecting sour skin (*Burkholderiacepacia*)-infected onions. *Journal of Food Engineering, 109*(1), 38–48.

Wold, J. P., Jakobsen, T., & Krane, L. (1996). Atlantic salmon average fat content estimated by near-infrared transmittance spectroscopy. *Journal of Food Science, 61*, 74–77.

Wold, S., Sjostrom, M., & Eriksson, L. (2001). PLS-regression: a basic tool of chemometrics. *Chemometrics and Intelligent Laboratory Systems, 58*, 109–130.

Workman, J. R. J. J., Mobley, P. R., Kowalski, B. R., & Bro, R. (1996). Review of chemometrics applied to spectroscopy: 1985–98, Part 1. *Applied Spectroscopy Reviews, 31*, 73–124.

Wu, D., Sun, D.-W., & He, Y. (2012a). Application of long-wave near infrared hyperspectral imaging for measurement of color distribution in salmon fillet. *Innovative Food Science & Emerging Technologies, 16*, 361–372.

Wu, D., Shi, H., Wang, S., He, Y., Bao, Y., & Liu, K. (2012b). Rapid prediction of moisture content of dehydrated prawns using online hyperspectral imaging system. *Analytica Chimica Acta, 726*, 57–66.

Wu, D., Wang, S., Wang, N., Nie, P., He, Y., Sun, D.-W., & Yao, J. (2013). Application of time series hyperspectral imaging (TS-HSI) for determining water distribution within beef and spectral kinetic analysis during dehydration. *Food and Bioprocess Technology*. doi:10.1007/s11947-012-0928-0.

Wu, D., & Sun, D.-W. (2013). Potential of time series-hyperspectral imaging (TS-HSI) for non-invasive determination of microbial spoilage of salmon flesh. *Talanta, 111*, 39–46.

Wu, J., Peng, Y., Li, Y., Wang, W., Chen, J., & Dhakal, S. (2012c). Prediction of beef quality attributes using VIS/NIR hyperspectral scattering imaging technique. *Journal of Food Engineering, 109*(2), 267–273.

Ye, S. F., Wang, D., & Min, S. G. (2008). Successive projections algorithm combined with uninformative variable elimination for spectral variable selection. *Chemometrics and Intelligent Laboratory Systems, 91*(2), 194–199.

Zhang, X., & He, Y. (2013). Rapid estimation of seed yield using hyperspectral images of oilseed rape leaves. *Industrial Crops and Products, 42*, 416–420.

Zhu, F., Zhang, D., He, Y., Liu, F., & Sun, D. W. (2012). Application of visible and near infrared hyperspectral imaging to differentiate between fresh and frozen–thawed fish fillets. *Food and Bioprocess Technology*. doi:10.1007/s11947-012-0825-6.

Zou, X., Zhao, J., Malcolm, J. W. P., Mel, H., & Mao, H. (2010a). Variables selection methods in near-infrared spectroscopy. *Analytica Chimica Acta, 667*(1–2), 14–32.

Zou, X., Zhao, J., Mao, H., Shi, J., Yin, X., & Li, Y. (2010b). Genetic algorithm interval partial least squares regression combined successive projections algorithm for variable selection in near-infrared quantitative analysis of pigment in cucumber leaves. *Applied Spectroscopy, 64*(7), 786–794.